Atmospheric Environment 199 (2019) 233–243

Contents lists available at ScienceDirect

Atmospheric Environment

journal homepage: www.elsevier.com/locate/atmosenv

# A new method for assessing the efficacy of emission control strategies

Huiying Luo[a], Marina Astitha[a,*], Christian Hogrefe[b], Rohit Mathur[b], S. Trivikrama Rao[a,c]

[a] University of Connecticut, Department of Civil and Environmental Engineering, Storrs-Mansfield, CT, USA
[b] U.S. Environmental Protection Agency, Research Triangle Park, NC, USA
[c] North Carolina State University, Raleigh, NC, USA

ARTICLE INFO

*Keywords:*
Ozone
Air quality models
Emission control strategies
Attainment demonstration
Probability of exceeding the standard
Time series analysis

ABSTRACT

Regional-scale air quality models and observations at routine air quality monitoring sites are used to determine attainment/non-attainment of the ozone air quality standard in the United States. In current regulatory applications, a regional-scale air quality model is applied for a base year and a future year with reduced emissions using the same meteorological conditions as those in the base year. Because of the stochastic nature of the atmosphere, the same meteorological conditions would not prevail in the future year. Therefore, we use multi-decadal observations to develop a new method for estimating the confidence bounds for the future ozone design value (based on the 4th highest value in the daily maximum 8-hr ozone concentration time series, DM8HR) for each emission loading scenario along with the probability of the design value exceeding a given ozone threshold concentration at all monitoring sites in the contiguous United States. To this end, we spectrally decompose the observed DM8HR ozone time series covering the period from 1981 to 2014 using the Kolmogorov-Zurbenko (KZ) filter and examine the variability in the relative strengths of the short-term variations (induced by synoptic-scale weather fluctuations; referred to as synoptic component, SY) and the long-term component (dictated by changes in emissions, seasonality and other slow-changing processes such as climate change; referred to as baseline component, BL). Results indicate that combining the projected change in the ozone baseline level with the adjusted synoptic forcing in historical ozone observations enables us to provide a probabilistic assessment of the efficacy of a selected emissions control strategy in complying with the ozone standard in future years. In addition, attainment demonstration is illustrated with a real-world application of the proposed methodology by using air quality model simulations, thereby helping build confidence in the use of regional-scale air quality models for supporting regulatory policies.

## 1. Introduction

In the United States, regional-scale air quality models are used to design emission controls needed to comply with the ozone standard (i.e., the design value, defined as the 4th highest daily maximum 8-h ozone concentration in each year averaged over a consecutive 3-year period, to not exceed a specified level). Year-to-year changes in ozone air quality over the contiguous United States (CONUS) are attributable to variations in meteorological conditions, local-to-hemispheric scale emissions loadings and factors such as stratospheric-tropospheric exchanges and climate change. In current regulatory applications, a regional air quality model is applied for a base year and a future year with reduced emissions using the same meteorological conditions as those in the base year. According to the current recommended modeling guidance, the observed base year design value is multiplied by the ratio of the average of the top 10 modeled ozone concentrations for the base and future years to assess whether the estimated future year design value meets the ozone standard (U.S. EPA, 2014). Hence, with the current methodology, we would not know how the variability in meteorological conditions affects the efficacy of emission reduction policies in assuring compliance with the ozone standard in the future year. Also, because the same meteorological conditions as those in the base year would not prevail in future years and observations for the future year are not available, the current attainment demonstration methodology can never be evaluated relative to observations.

Past studies have revealed that the absolute levels of ozone concentrations simulated by regional-scale air quality models can be subject to significant bias and errors (Schere et al., 2012; Hogrefe et al., 2014; Gilliam et al., 2015; Porter et al., 2015, 2017; Astitha et al., 2017; Emery et al., 2017; Henneman et al., 2017; Solazzo et al., 2017a, b). This is particularly true at the upper tail of the concentration distribution (Hogrefe et al., 2014; Porter et al., 2015). Astitha et al. (2017) evaluated the year-to-year changes in ozone air quality induced by variations in meteorology and emissions during 1990–2010 using spectral decomposition of both observed and WRF-CMAQ simulated

* Corresponding author. Civil and Environmental Engineering, University of Connecticut, 261 Glenbrook Road, Storrs, CT, USA.
*E-mail address:* marina.astitha@uconn.edu (M. Astitha).

https://doi.org/10.1016/j.atmosenv.2018.11.010
Received 26 April 2018; Received in revised form 26 September 2018; Accepted 5 November 2018
Available online 09 November 2018
1352-2310/ © 2018 Elsevier Ltd. All rights reserved.

daily maximum 8-hr ozone concentration time series with the objective of identifying the underlying forcing mechanisms that control ozone exceedances. Analysis of the information embedded in the daily maximum 8-hr ozone time series from the past few decades reveals that the long-term forcing, which is attributable to the emissions loading on local-to-hemispheric scales, climate change, variations in the stratospheric-tropospheric exchange processes, and the short-term forcing, which is attributable to synoptic-scale weather fluctuations, are to be viewed as the necessary and sufficient conditions, respectively, for controlling the ozone exceedances (Rao et al., 1996, 2011; Hogrefe et al., 2000; Porter et al., 2017; Astitha et al., 2017).

To help improve upon the current method for using regional air quality models in the regulatory context, we analyzed 34 years of ozone observations (1981–2014) having at least 80% data coverage over the contiguous United States. The main objectives of this study are to 1) develop a method for estimating the confidence bounds for the projected ozone design value (DV), and 2) demonstrate how future projections could be communicated in a probabilistic framework that explicitly accounts for the prediction uncertainties stemming from the year-to-year variability in meteorology. We examine the variability in observed extreme values stemming from changes in emissions and meteorology during the 1981–2014 time period and present a new method for building confidence when regional-scale air quality models are used for policy support. This new probabilistic method for assessing the efficacy of emission control strategies and ozone data employed are described in Section 2, and evaluated in Section 3. Attainment demonstration in a real-world application using the suggested method and the CMAQ model is discussed in Section 4. Summary and conclusions are presented in Section 5.

## 2. Data and methods

### 2.1. Ozone measurements and CMAQ simulations

Ground-level daily maximum 8-hr ozone concentration (DM8HR) observations during May to September covering the contiguous United States (CONUS) were obtained from the U.S. Environmental Protection Agency's (EPA) Air Quality System (AQS). A valid ozone season consists of at least 80% data coverage during May to September at each station. A total of 156 stations with at least 30 valid years (to provide enough synoptic conditions, noted as 30 + in this paper) from 1981 to 2014 were analyzed.

Two sets of WRF/CMAQ model simulations covering the CONUS for the year 2010 were employed to demonstrate this new approach from the regulatory perspective. These simulations were performed as part of the third phase of the Air Quality Model Evaluation International Initiative (AQMEII3). The first simulation, hereafter referred to as BASE, uses meteorology, emissions, and lateral boundary conditions representative of 2010 conditions, whereas the second simulation, hereafter referred to GLO, reflects to a 20% reduction of anthropogenic emissions loading both in the global model simulations providing lateral boundary conditions and within the WRF/CMAQ modeling domain while using the same 2010 meteorology as in BASE. A detailed description of the AQMEII3 modeling scenarios can be found in Galmarini et al. (2017). Further details on the configuration of the WRF/CMAQ system can be found in Hogrefe et al. (2018). Model evaluation results for the BASE simulation can be found in Solazzo et al. (2017a, b) and Hogrefe et al. (2018). These two simulations are representative of how an air quality model is used by the regulatory agencies for attainment demonstration.

### 2.2. Kolmogorov-Zurbenko (KZ) filter

In this study, we examine the year-to-year variability in the relative strengths of the short-term component induced by synoptic-scale weather fluctuations (SY) and the magnitude of the long-term component (BL) induced by changes in anthropogenic emissions and non-anthropogenic background ozone, and other longer-term factors embedded in observed ozone time series during 1981–2014. This is accomplished by decomposing the May–September DM8HR with the Kolmogorov-Zurbenko (KZ) low-pass filter, a commonly-used filter to separate various temporal signals (Rao and Zurbenko, 1994; Rao et al., 1995, 1997; Eskridge et al., 1997; Milanchus et al., 1998; Gardner and Dorling, 2000; Ibarra-Berastegi et al., 2001; Hogrefe et al., 2003; Vukovich and Sherwell, 2003; Maxwell-Meier and Chang, 2005; Wise and Comrie, 2005a, b; Yang and Zurbenko, 2010; Galmarini et al., 2013; Kang et al., 2013; Sá et al., 2015; Phalitnonkiat et al., 2016; Zhang et al., 2018; Zurbenko and Smith, 2018).

The KZ($m$,$k$) filter is defined as $k$ applications of a simple moving average of $m$ points. The moving average can be defined as follows:

$$Y(t) = \frac{1}{m} \sum_{s=-(m-1)/2}^{(m-1)/2} X(t+s) \tag{1}$$

where time series Y($t$) is the long-term component of time series X($t$), m is the window length of the filter. The process is repeated k times by using Y(t) in the previous step as X($t$) in the next iteration. The window length ($m$) and the number of iterations ($k$) together determine the scale separation between the frequencies present in the long-term component and those present in the residual short-term component (original time series – final longer-term component). An analytical representation of the filter transfer function that can be used to calculate the separation frequency for a given combination of m and k can be found in Rao et al. (1997) and a comparison against other spectral decomposition approaches is provided in Hogrefe et al. (2003).

The 50% cutoff frequency of the KZ filter, meaning the energy at this frequency is separated half-half by the KZ(m,k), can be expressed as (see Rao et al., 1997 for details on filter characteristics):

$$\omega_0 \approx \frac{\sqrt{6}}{\pi} \sqrt{\frac{1 - 0.5^{1/(2k)}}{m^2 - 0.5^{1/(2k)}}} \tag{2}$$

The parameters of the KZ filter are selected based on the scale of synoptic events, which is 2–21 days (Eskridge et al., 1997; Hogrefe et al., 2001). Slow variations with period of longer than about 3 weeks in the signal should go into BL component. We use KZ(5, 5) with window length of m = 5 days and k = 5 iterations to decompose May–September time series of observed and simulated daily maximum 8-hr ozone concentrations into the short-term synoptic (SY) and long-term baseline (BL) components for each year (Porter et al., 2015; Hogrefe et al., 2000; Astitha et al., 2017). The 50% cutoff frequency for KZ(5,5) is 0.0411, which gives a cutoff period for daily sampling of 1/0.0411 ≈ 24 days. The decomposition can be expressed as:

$$BL(t) = KZ(5,5) \tag{3}$$

$$SY(t) = O_3(t) - KZ(5,5) \tag{4}$$

where t = 1, 2, …, 153 denotes the days from May 1st to September 30th, $O_3$ (t) is the original time series of observed DM8HR ozone concentrations (the orange $O_3$ in Fig. 2a for instance), BL(t) is the baseline or long-term component (the red BL in Fig. 2a) and SY(t) is the residual short-term component.

An example of the spectral decomposition of 2014 DM8HR at Stratford, CT (Fig. 1a) and the power spectrum (Fig. 1b) of corresponding time series illustrated below reveals that there is good separation between the two forcings at around 24 days with some leakage of information present. Since we are dealing with non-linear and non-stationary ozone time series, some leakage of information between the two separated components is expected.

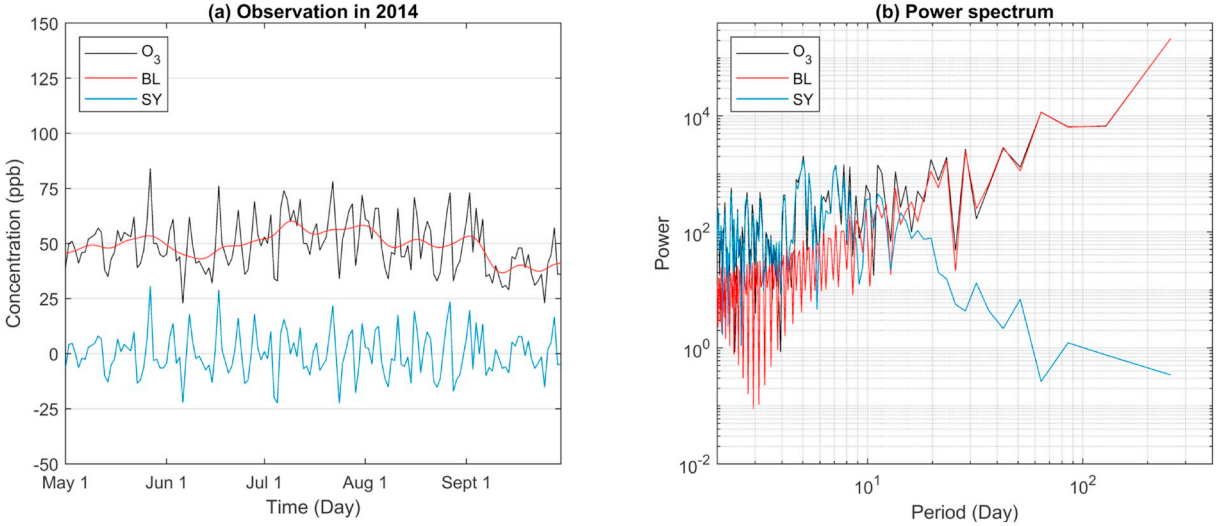


**Fig. 1.** KZ filter decomposition of observed ozone concentrations for Stratford, CT. (a) Ozone time series ($O_3$), baseline component (BL) and synoptic component (SY) in 2014. (b) Power spectrum of each component and the ozone concentration that designates the time period (in days) when the two components separate.

### *2.3. Ozone time series reconstruction and the importance of the baseline component*

Ozone time series reconstruction is accomplished by adding the synoptic and baseline components (Eq. (5)), a reverse process of the KZ decomposition described in the previous section. The ozone baseline component represents the ozone pollution that is created primarily by emission sources whereas the prevailing synoptic-scale meteorology controlling the regional-scale transport of ozone and its precursors is reflected in the synoptic component.

$$O_3\ (t) = SY(t) + BL(t) \tag{5}$$

A linear relationship between the strength of the synoptic forcing, defined as the standard deviation of the weather-induced variations in ozone time series data (SYstd) and the mean of the baseline concentration (BLmean) has been found at each monitoring site in CONUS; an example of this linear relationship between BLmean and SYstd is illustrated in Fig. S1.

$$SYstd = f(BLmean) = p * BLmean + q \tag{6}$$

Given the high correlation between the strength of the synoptic forcing and the magnitude of the baseline concentration (Porter et al., 2017; Astitha et al., 2017), each observed synoptic component SY($t$) is adjusted according to the mean of a future BL using the relationship below before being superimposed (for example, if we want to reconstruct $O_3$ concentration for 2010 (*future*) with the synoptic component of year 1998 ($y$), we need to adjust the synoptic component with the BL of 2010):

$$SY_{y,\,adj}(t) = SY_y(t) * \frac{f(BLmean_{future})}{f(BLmean_y)} \tag{7}$$

in which y can be 1981,1982 … 2014, indicating the year of which the synoptic forcing is decomposed from (e.g. 1998 in the example given above). The future BL can be any baseline of interest (e.g. BL for the year 2010 in the example given above). The daily ozone concentration is then reconstructed by using the daily values of BL and $SY_{adj}$:

$$O_3^{y,future}(t) = BL_{future}(t) + SY_{y,adj}(t) \tag{8}$$

An example of the decomposition and reconstruction is shown in Fig. 2, where the observed DM8HR time series from May through September in 2002 and 2014, along with the embedded baseline concentration in Stratford, CT are illustrated. There has been a substantial improvement in ozone air quality between 2002 and 2014, likely due to the implementation of emission control programs on the electric generation units and motor vehicles that helped significantly reduce emissions of NOx and VOCs; the meteorological conditions including daily precipitation, average wind speed, mean and maximum temperature between 2002 and 2014 are not significantly different. This substantial improvement is indicated by the reduction in the 4th highest ozone concentration from 103 ppb in 2002 to 74 ppb in 2014 and a reduction in the number of days exceeding the 2008 NAAQS standard (75 ppb) from 27 in 2002 to only 3 in 2014 (Fig. 2a and b). The large reduction in the baseline concentration as well as the temporal variability of the baseline concentration within the same year is evident.

To illustrate the relative importance of changes in the baseline vs. variability in the strength of the synoptic forcing, we reconstructed the ozone time series by adding the adjusted 2014 synoptic forcing to the 2002 baseline forcing (Fig. 2c) and vice versa (Fig. 2d). Combining the higher baseline in 2002 with the synoptic forcing that prevailed in 2014, we see that the 4th highest ozone changed from 103 to 95 ppb and the number of exceedance days changed from 27 to 23, whereas combining the lower baseline in 2014 with the 2002 synoptic forcing led to 80 ppb (instead of 74 ppb) for the 4th highest ozone and changed the number of exceedances from 3 to 4. Thus, the increase seen in the number of ozone exceedances is primarily influenced by the baseline level and not by changes in the synoptic forcing. Similar results were found when different years and stations were used without the adjustment for the synoptic component (see Rao et al., 2011).

The above conclusions are further supported if we expand the experiment to superimpose 34 years of synoptic forcings on the baselines that prevailed in 2002 and 2014 for the same Stratford, CT station (Fig. 2e and f). It is evident that the 4th highest ozone concentrations associated with a given baseline (BL) can vary depending upon the prevailing synoptic forcing (see crosses in Fig. 2e and f denoting the 4th highest for each "reconstructed" year), but these variations are much smaller than the differences seen between the magnitudes of baselines in 2002 and 2014. Moreover, the position of the crosses in these time series (Fig. 2e and f) also indicates that the 4th highest values associated with 30 + years of synoptic forcing tend to cluster together in time and coincide with times when the baseline level reaches a local maximum, further emphasizing the notion that elevated baseline levels are necessary for observing ozone exceedances.

Reconstruction of ozone time series using the observed BL in 2002 and 34 years of SY (Fig. 2e) yields 34 values of the 4th highest ozone concentrations, one from each reconstructed ozone time series (Eq. (8)). This allows the determination of the 95% confidence bound for the 4th highest (*CBs*, defined by the 2.5th and 97.5th percentile values of the distribution; more details are provided in Section 2.4) as 94–114 ppb

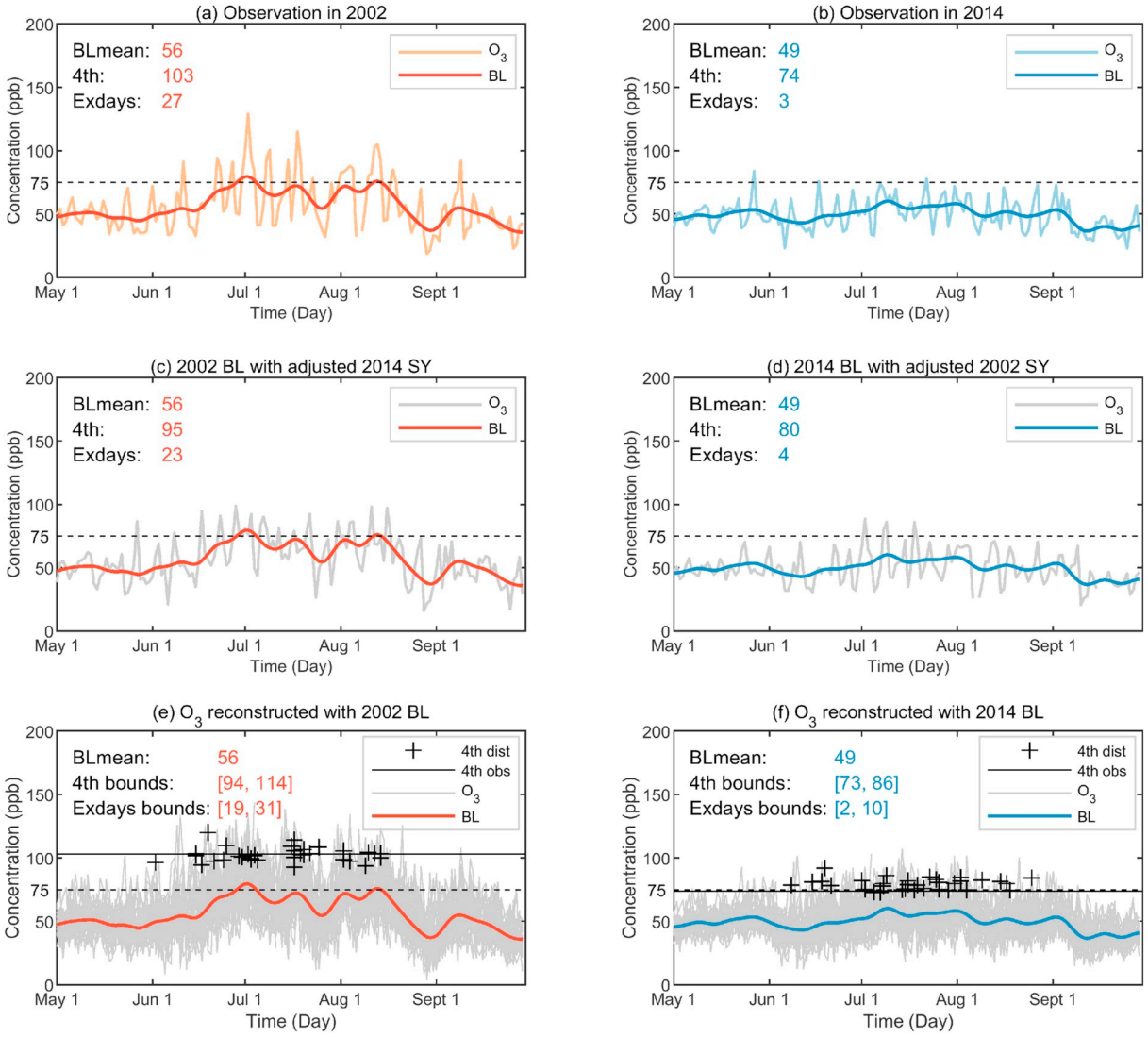


**Fig. 2.** Observed ozone time series ($O_3$) and long-term forcing (BL) along with the 4t highest ozone concentration and number of ozone exceedances at Stratford, CT during May–September: (a) 2002; (b) 2014; (c) reconstruction of $O_3$ using 2002 BL and adjusted 2014 synoptic forcing (SY); (d) reconstruction of $O_3$ using 2014 BL and adjusted 2002 SY. Reconstructed ozone $O_3$ by superimposing different synoptic forcings from 34 years on the same baseline concentration in: (e) 2002 (95% confidence bounds of the 4th highest: 94–114 ppb, actual = 103 ppb); (f) 2014 (95% confidence bounds of the 4th highest: 73–84 ppb, actual = 74 ppb). Crosses in (e–f) denote the 4th highest ozone concentrations with the 34 different synoptic conditions and the solid straight black line the observed 4th highest ozone concentration with respect to the baseline year.

with the actual observed being 103 ppb; similarly, the 95% *CBs* for the number of exceedance days are 19–31 with 27 being observed. Likewise, 95% *CBs* for the 4th highest ozone concentrations with the 2014 BL (Fig. 2f) is 73–86 ppb with the observed being 74 ppb and the number of exceedances is 2–10 with the actual being 3. Comparing the influence of the two baseline forcings, it is evident that the baseline with the higher magnitude in 2002 (Fig. 2e) yields higher 4th highest ozone concentrations than those in 2014 (Fig. 2e and f) with 34 years of possible synoptic forcings. Analysis like that presented in Fig. 2 is given for four additional sites in the supplemental material (Figs. S2–S5) and the conclusions are identical to those discussed for Stratford, CT. This analysis demonstrates that change in the baseline level induced by emission reduction rather than differences in the meteorology is the main driver for improvements seen in ozone air quality between 2002 and 2014. The above results indicate that the magnitude of the baseline concentration dictates the peak ozone levels that can be reached for a given synoptic forcing, further validating the conclusions reached in previous studies (Rao et al., 2011; Astitha et al., 2017; Porter et al., 2017).

### 2.4. Estimating confidence bounds

It should be noted that the 4th highest concentration (or any other extreme value) in any given year is a single event out of a population; that is, even if emissions were to remain the same, stochastic variations and meteorological conditions in a different year could lead to a different 4th highest ozone concentration. From a statistical perspective, an observation on any given day represents a single realization out of an unknown underlying distribution. Therefore, it is important to characterize and quantify the distribution of the possible future 4th highest ozone concentrations and design values associated with each emissions loading scenario, instead of relying on a single value (Pinder et al., 2009). Once the distribution of the 4th order statistic is determined, it is possible to estimate the 95% confidence bounds for the 4th highest ozone concentration. This can be done using various methods: 1) extreme value theory (EVT) based on its parent DM8HR ozone time series, 2) $\mu$ (mean) $\pm$ 2$\sigma$ (standard deviation) provided that those 30+ 4th highest values are normally distributed or 3) the 2.5th percentile and 97.5th percentile values of the variable distribution based on bootstrapping.

The first approach, the extreme values theory (EVT), provides the theoretical framework to estimate the distribution of any extreme values of interest, say, the 4th highest value for ground level ozone for this study, from the underlying DM8HR ozone time series (Gumbel, 1958; Roberts, 1979; David, 1981; Chock, 1984; Rao et al., 1985; Hogrefe and Rao, 2001). However, the application of the exact theory of extreme values relies on the knowledge of the analytical form of the underlying DM8HR ozone distribution, which is generally unclear (Gumbel, 1958; Roberts, 1979; David, 1981; Chock, 1984; Rao et al., 1985; Hogrefe and Rao, 2001). It has been shown that the analytical cumulative distribution function (CDF) of the upper tail of most parent distributions can be described by an exponential distribution:

$$F(x) = 1 - e^{-\lambda(x-B)} \tag{9}$$

where λ and B are the shape and location parameters, respectively,

$$\lambda = \left[\frac{1}{n-1} \times \sum_{i=1}^{n} (x_{(i)} - x_{(n)})\right]^{-1} \tag{10}$$

$$B = x_{(n)} \tag{11}$$

in which, x is the upper 20% of the ozone concentration distribution at any given site in one specific year and n is the number of observations in x (n ranges from 24 to 31 years in this study, which is 20% of valid days during 153 days of May–September); x(1), x(2), …, x(n) are the highest, second-highest, …, smallest of the n tail values, respectively.

The exact theory of extreme values can then be applied to estimate the CDF of the 4th order statistic (i.e., the 4th highest ozone concentration) from the following expression:

$$G(x) = \sum_{j=0}^{3} \binom{n}{j} \times [1 - F]^{j} \times [F]^{n-j} \tag{12}$$

The 95% confidence bounds for the 4th highest ozone is determined by the 2.5th and 97.5th percentiles from the CDF G(x).

The first method of calculating the confidence bounds using the EVT, is not applicable to the design value since it requires averaging the 4th highest ozone value over a consecutive 3-year period. However, it can serve to validate the confidence bounds derived from historical ozone observations described in Section 3.1. The second method (mean ± 2 times the standard deviation) requires the 4th highest ozone concentrations to be normally distributed, which may not be valid in all cases. Therefore, we utilize the bootstrap method (i.e., resampling with replacement) to develop the distribution of design values by randomly drawing the 30 + synoptic conditions 2000 times to represent the stochastic variation of synoptic conditions among the 3 consecutive years and utilize the same manner for 4th highest (the 2000 random samples are to be considered as bootstrap estimates).

### 2.5. Probabilistic assessment of emission control strategies using the baseline projection method based only on observations

In the following, we discuss the development and details of the proposed baseline projection methodology, described step by step in Fig. 3, to assess ozone extreme values for a given emissions loading scenario under varying meteorological conditions based on 30 + years of ozone observations in CONUS. As noted before, time series of the DM8HR ozone concentrations during May to September at each site are spectrally decomposed into the baseline and synoptic components with the KZ filter for all years as in Fig. 1a.

Given the importance of the baseline level discussed in Section 2.3, we propose to use the Baseline Projection Method to construct the baseline component for the future by projecting the base year observed daily BL onto a future year by performing linear regression of rank-ordered base and future year baseline concentrations. In Step 1 of Fig. 3, *a* and *b* are slope and intercept of the linear regression between the rank-ordered base year's and future year's BL. In real-world applications (i.e., ozone attainment demonstration) where future observations are not available, *a* and *b* are determined from the CMAQ model simulations of base year's and emissions control scenario's BL. $BL_{future,\ proj}$ is the projected future BL from the observed base year's BL ($BL_{base,obs}$). As an example, baseline linear regression for Stratford is shown (observed baselines are used here to demonstrate the method) in Fig. 4a and the 2014 projected baseline component is the green solid line in Fig. 4b, which is projected from the observed 2002 baseline as in Fig. 2a. This process is repeated for two additional pairs of base and future years to obtain a total of three years of projected BL time series given the need of 3-year averaging for the calculation of the design value (step 2, Fig. 3).

Regression on rank-ordered ozone baseline concentration is necessary when we use only observations in Step 1 since it helps to eliminate the influence of changing meteorological conditions imbedded in observations in base and future years as well as the weekday-weekend differences and holidays between the two years; high or low ozone concentrations tend to occur under similar meteorological conditions for any given year, thereby permitting examination of the change in the ozone baseline induced predominantly by changing emissions. Since model projections use the same meteorology as in the base year, adding the difference between the base and future year baselines to the base year BL for each day works equally well.

In Step 2, ozone time series are reconstructed by adding the projected BL to the 30 + historically observed synoptic components adjusted for the specific baseline level, providing sufficient information to develop the possible distribution of the 4th highest and the design value (DV). That way, the distribution of the 4th highest and the DVs are generated for the future year by 2000 bootstrap replications to represent the stochastic variability in synoptic forcing (each projection, shown as (A) is Fig. 3, generates 34 values of the 4th highest; to formulate the DV distribution we take the 3-yr average of the 4th highest; instead of selecting a-priori the 3-yr average, e.g. $4th_{1981,2012} + 4th_{1981,2013} + 4th_{1981,2014}$, we introduce bootstrapping for the random selection of the synoptic year). In Step 2 of Fig. 3, $SY_{y,\ adj}$ represents the $BL_{future,\ proj}$ adjusted SY from year *y* (*y*th year in 1981–2014) and $O_3^{y,\ future}$ is the corresponding reconstructed DM8HR time series. The possible 4th highest values from the multiple reconstructed time series in 2014 for Stratford are marked as crosses in Fig. 4b.

Once the distribution of the 4th highest ozone or the design value is estimated, the confidence bounds (*CBs*) and probability of the 4th highest ozone or the design value exceeding a given threshold (*Pex*), say, the 2008 NAAQS standard pf 75 ppb, can be estimated for a given year or emissions loading scenario. In Step 3 of Fig. 3, *CBs* represent the 95% confidence bounds and *Pex* the probability of DV exceeding the NAAQS ozone standard. Consequently, *CBs* for ozone exceedances for 2014 at Stratford using the Baseline Projection Methodology (observations-based analysis only) is 73–88 ppb for the 4th highest and 3–10 for the number of days with exceedances (Fig. 4b), well-resembling the results when the observed baseline is used (Fig. 2f). Again, the actual ozone measurements fall within the estimated confidence bounds (actual 4th highest 74 ppb, actual exceedance days 3).

This exercise illustrates the methodology for the BL projection and probabilistic approach for predicting the 4th highest ozone concentration and number of ozone exceedances. A more comprehensive evaluation of the proposed method will be presented in the following section. It should be noted that since the time series of DM8HR for a future year is reconstructed, parameters such as median DM8HR can also be derived in a similar manner.

## 3. Results and discussion

The use of multi-year ozone observations rather than model simulations in this section demonstrates the appropriateness of the proposed method without having to delve into the impacts of model performance

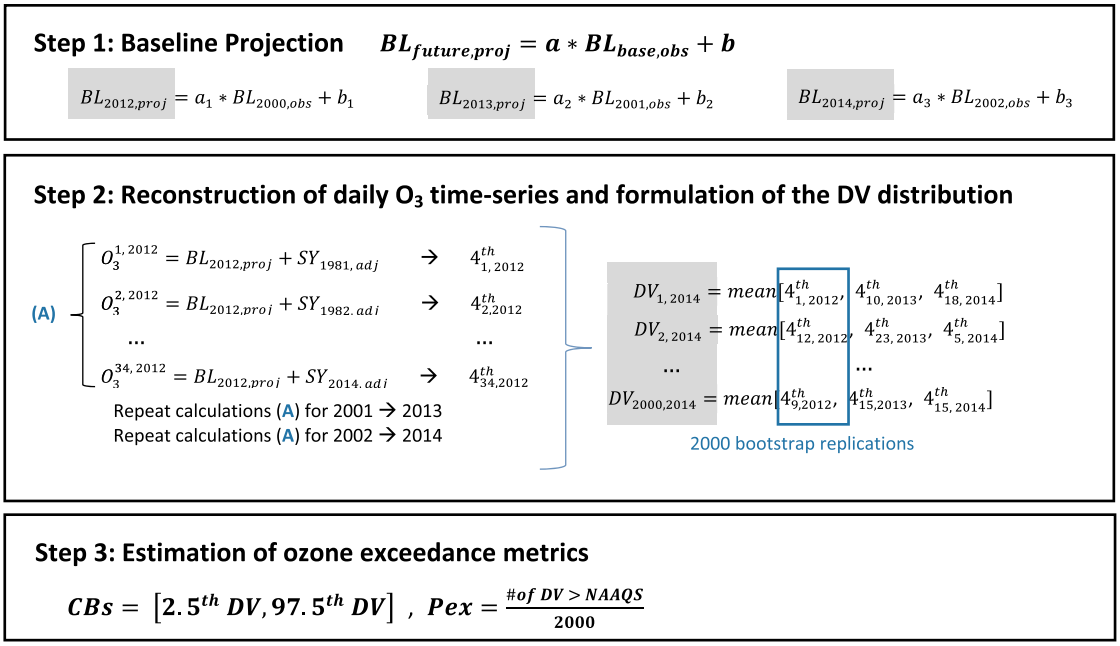
Step 1: Baseline Projection $BL_{future,proj} = a * BL_{base,obs} + b$
$BL_{2012,proj} = a_1 * BL_{2000,obs} + b_1$
$BL_{2013,proj} = a_2 * BL_{2001,obs} + b_2$
$BL_{2014,proj} = a_3 * BL_{2002,obs} + b_3$
Step 2: Reconstruction of daily $O_3$ time-series and formulation of the DV distribution
(A)
$O_3^{1,2012} = BL_{2012,proj} + SY_{1981,adj} \rightarrow 4^{th}_{1,2012}$
$O_3^{2,2012} = BL_{2012,proj} + SY_{1982,adj} \rightarrow 4^{th}_{2,2012}$
...
$O_3^{34,2012} = BL_{2012,proj} + SY_{2014,adj} \rightarrow 4^{th}_{34,2012}$
Repeat calculations (A) for 2001 → 2013
Repeat calculations (A) for 2002 → 2014
$DV_{1,2014} = mean[4^{th}_{1,2012}, 4^{th}_{10,2013}, 4^{th}_{18,2014}]$
$DV_{2,2014} = mean[4^{th}_{12,2012}, 4^{th}_{23,2013}, 4^{th}_{5,2014}]$
...
$DV_{2000,2014} = mean[4^{th}_{9,2012}, 4^{th}_{15,2013}, 4^{th}_{15,2014}]$
2000 bootstrap replications
Step 3: Estimation of ozone exceedance metrics
$CBs = [2.5^{th}\ DV, 97.5^{th}\ DV]$ , $Pex = \frac{\#of\ DV > NAAQS}{2000}$

**Fig. 3.** Representation of the proposed probabilistic assessment of emission control strategies with the Baseline Projection Method. BL = baseline forcing; base = base year; future = future year; SY = synoptic forcing. Example of a 12-yr projection is given (2002–2014). In step 2 the ozone time series is estimated by $O_3^{y,future} = BL_{future,proj} + SY_{y,adj}$ with y denoting the years of available observations (1 = 1981 to 34 = 2014). Detailed description of each step is given in the text (section 2.5).

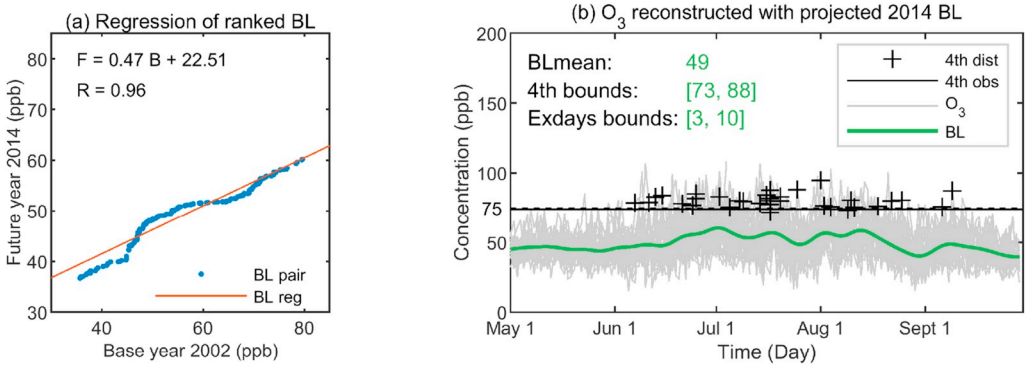


**Fig. 4.** Baseline projection from 2002 to 2014 at Stratford, CT. (a) Rank-ordered observed baseline regression between base year 2002 and future year 2014 ($a = 0.47, b = 22.51$); (b) Reconstructed ozone for 2014 by using the projected 2014 BL from the 2002 BL based on their regression relationship in (a) and 34 years of SY forcings. Crosses denote the 4th highest ozone concentrations during the 34 synoptic years and the straight black line the observed 4th highest ozone concentration in 2014.

in reproducing the BL concentration and changes in the BL stemming from emissions reductions. Furthermore, it lends credence to the proposed method since observation-based analysis can be validated. This enables comparison of the estimated confidence bounds for 2007 to 2014 projections against actual observed ozone design values. We selected projections that span at least 5 years to allow sufficient time for changes in emissions from emission control policies to become apparent. The main reason that the projections are focused from 2000 onward, is that the 4th highest observed ozone trends in the earlier decade (namely, 1990–2000) have been shown to be not statistically significant (Astitha et al., 2017; Porter et al., 2017; Guo et al., 2018), whereas the ozone trends during 2000–2010 are statistically significant and we wanted to demonstrate the BL projection method in a period covering significant changes in ozone exceedances driven primarily by emission changes.

### 3.1. Width of the 95% confidence bound

The exact theory of extreme values (EVT) provides the theoretical framework to examine the appropriateness of the proposed method to estimate confidence bounds of 4th highest values. The EVT method estimates the confidence bounds of the extreme value (4th highest in this application) directly from the future observed DM8HR time series, accounting for its statistical property. Thus, it is treated here as the ground truth. These two *CBs* (from EVT and the proposed BL method) are not expected to be identical since they are based on different mathematical approaches and statistical assumptions; nevertheless, they should be of similar magnitude.

The width of *CBs* for the 4th highest ozone calculated from the proposed method over all stations in CONUS is very similar to that estimated by the EVT (Fig. 5; box plots show the spatial distribution of the *CBs* width). The range of 10–15 ppb derived from the proposed method is consistent with the magnitude of the width of *CBs* derived from the EVT method. In addition, there is a capability to project into the future year using a variety of base years since the estimated *CBs* for a specific future year from multiple different base years, with different projection intervals, yield very similar distributions (Fig. 5). When more years of historical observations than 34 considered here are included, we expect to see even better agreement between the widths of the CBs derived from the proposed method and EVT.

### 3.2. Are the observed design values within the estimated confidence bounds?

It is crucial for the "future year" observed design value to fall within the predicted 95% confidence bounds for a valid projection method. As

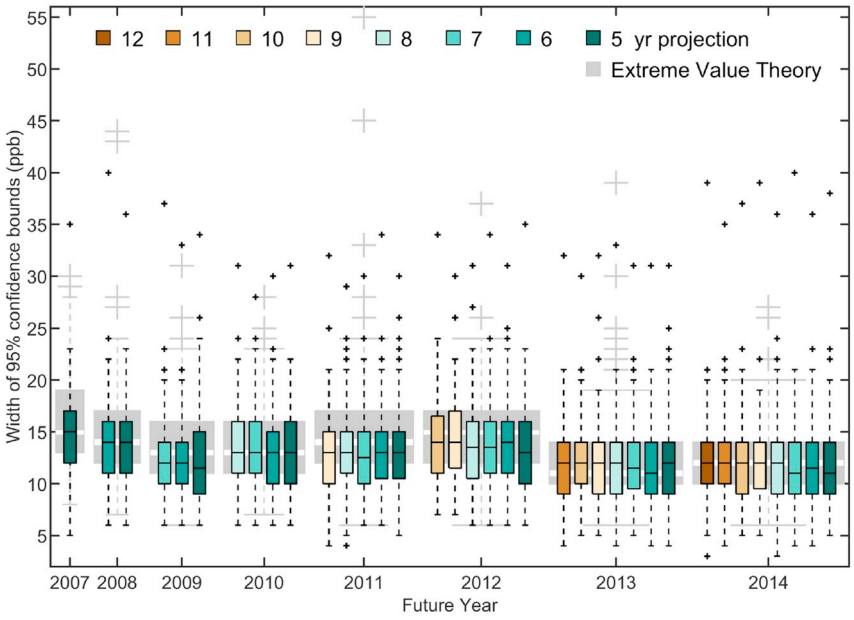


**Fig. 5.** Box plots of 95% Confidence Bounds (*CBs*) width for the 4th highest (in ppb) for multiple future projections (≥5yrs) and all stations (colored boxes denote different projection intervals in years). *CBs* width from the exact theory of extreme values (EVT) is shown with the grayscale background boxplots. Boxes are marked at 25th, 50$^{th}$, 75th percentile. Maximum whisker length equals 1.5 times the inter quantile range. Topmost outliers of *CBs* width in all projections come from one station at Pomona, CA.

shown in Fig. 6, a clear majority (92–99% of the sites) of the observed DVs fall within the estimated confidence bounds. There are few stations where the observed DV does not fall within the confidence bounds and those vary depending on the projected year. More than half of the unsuccessful cases are the result of rounding up of the DV and CB values, with an actual decimal bias of less than one ppb. Other than that, these cases generally occur near large water bodies for specific future years when few local extreme events elevated the observed DV remarkably, leading to an underestimation of the CBs. Although we accounted for data completeness by selecting only stations with at least 80% date coverage per ozone season, missing data still play a noticeable role and is one of the reasons to miss the observed DV at some stations. The success rates for all possible projections except the ones shown here are also in the 92–99% range. This high success rate, together with the fact that the widths of the confidence bounds for the 4th highest values are similar to those derived from the exact theory of extreme values, provides confidence regarding the reliability and appropriateness of the proposed methodology for the ozone attainment demonstration that would be based upon air quality modeling simulations in real-world future applications.

### 3.3. Probabilistic assessment of ozone exceedances

An important feature of the proposed method is its ability to provide probabilistic assessments of future exceedances of given ozone threshold concentration (National Ambient Air Quality Standards, NAAQS). This is possible through the construction of a potential DV (or 4th highest) distribution dictated by 30 + years of observed synoptic forcings influencing a given baseline ozone concentration (long-term forcing). The probability of non-attainment of the ozone standard is estimated by dividing the total projected DVs that are greater than the threshold by the size of sample pool used to formulate the DV distribution (2000 in the proposed approach, Fig. 3). The result is illustrated in Fig. 7, where the actual ozone attainment (DV > 75 ppb) in the binary form for 2014 (Fig. 7a) is contrasted against the probability of the DV exceeding the NAAQS, *Pex* (DV > 75 ppb) constructed with the actual observed 2014 baseline and the baseline projected from 2002 into 2014 (Fig. 7b and c). The probability of the DV exceeding the NAAQS is a good indicator of the attainment status and conveys additional information for stations when DV is close to the level of the NAAQS (Fig. 7a and b). The two maps with either the actual observed 2014 baseline (Fig. 7b) or the projected 2014 baseline (Fig. 7c) convey almost identical situations, validating the proposed BL projection methodology.

Information on the probability of exceedance for each station would allow decision makers to explore the effects of selecting different cut-off probabilities for reaching attainment across the domain. Having the option of a probabilistic assessment allows policy-makers to decide upon emissions control strategies informed by the range of possible attainment/non-attainment scenarios to choose from. This is discussed in more detail in the following section where the attainment demonstration procedure is illustrated for a real-world future year projection scenario.

## 4. Attainment demonstration using regional air quality modeling simulations

The probabilistic assessment using the baseline projection method has been illustrated and evaluated in the previous sections. The proposed method is adopted for regional air quality models, specifically the CMAQ model, in this section to help develop robust ozone control strategies. The current ozone NAAQS attainment demonstration method uses the ratio of the mean of the top 10 modeled ozone concentrations in the emission control case to those in the base case simulated by a regional air quality model (U.S. EPA, 2014). The observed base year design value (defined as three consecutive DVs, by considering weighted-average of five years 4th highest) is then multiplied by this ratio to determine whether that emission control case would reduce the design value to the level of the ozone standard. In those cases when the projected future design value is close to the NAAQS, more rigorous Weight of Evidence Analysis should be completed, such as supplemental trend analysis, diagnostic analysis and implementation of additional model simulations (U.S. EPA, 2014). If non-attainment is determined based on the current year design value, increasing emissions reduction cases are modeled until the design value is at or below the level of the standard. Because the meteorology used for the base year would never prevail for future emission control years, the impacts of emission reductions on extreme values of interest cannot be predicted perfectly even if the model and its input data were perfect. Hence, there is no guarantee that the envisioned emission control strategy will in fact lead to ozone compliance in future years with the current method. Therefore, we present an alternative approach where emission reduction scenarios are accompanied by confidence bounds and probabilities of exceedance that account for the ever-present uncertainties in the

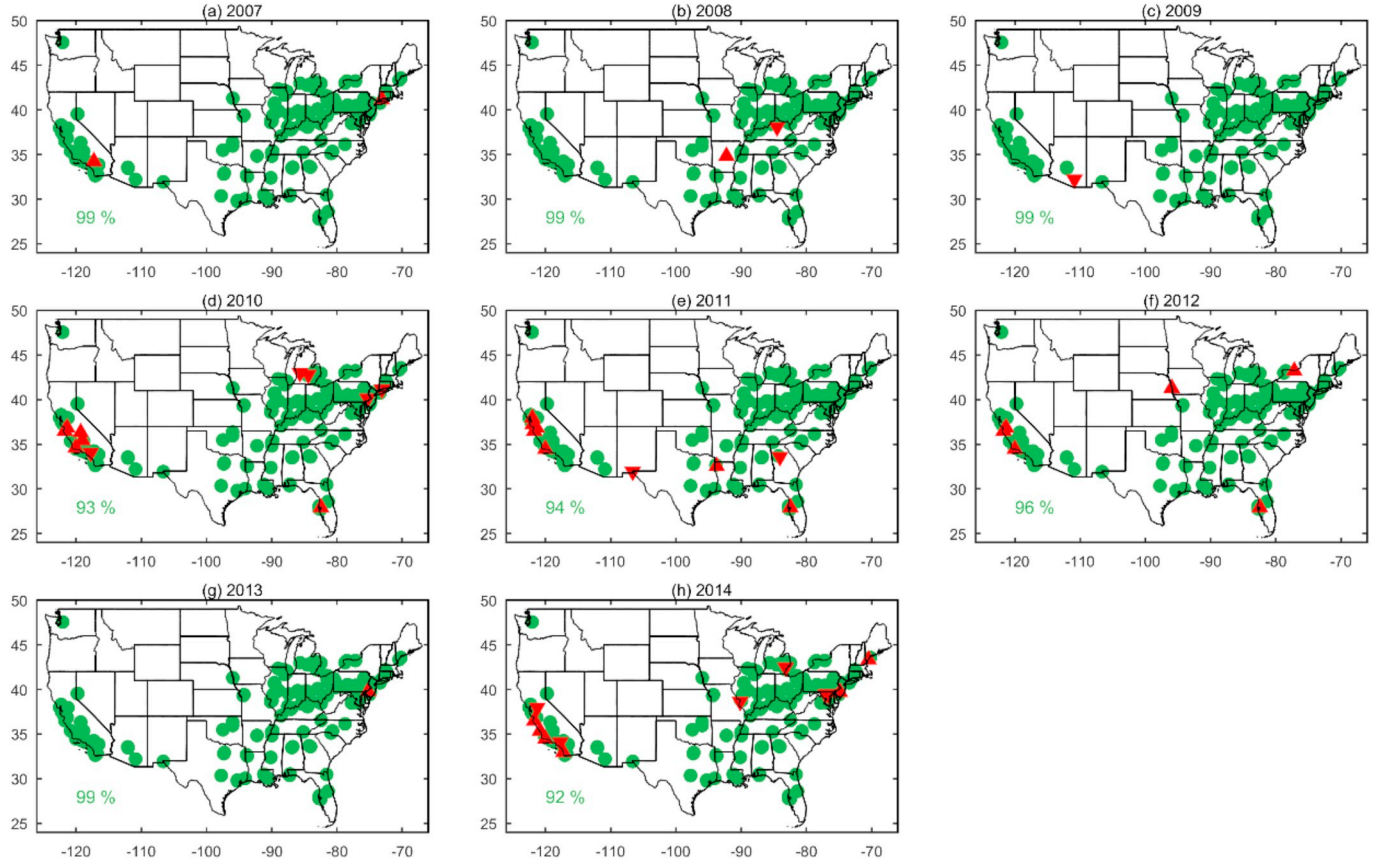


**Fig. 6.** Maps indicating whether the observed DV falls within the 95% confidence bounds calculated using the 5-yr projection for (a–h) 2007–2014. The colors in each subplot denote the observed DV relative to the estimated *CBs* at each station: Green circle = within the *CBs*; red triangle = outside the *CBs* (observed DV is higher than estimated CBs); red inverted triangle = outside the *CBs* (observed DV is lower than estimated CBs). (For interpretation of the references to color in this figure legend, the reader is referred to the Web version of this article.)

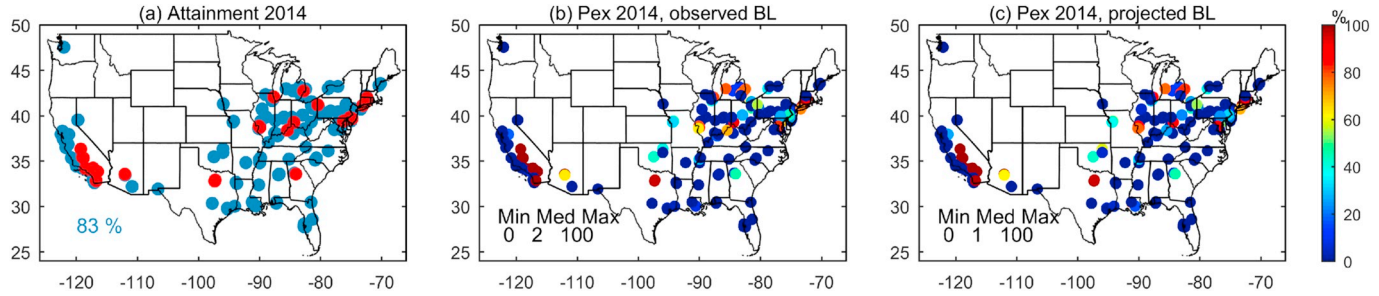


**Fig. 7.** Attainment determination. (a) Binary representation of ozone attainment status of observed 2014 DV (red = non-attainment, blue = attainment). (b) Probability of 2014 DV exceeding the ozone standard using the actual observed baseline. (c) Probability of projected 2014 DV exceeding the ozone standard using the proposed method over the 12-yr projection interval. (For interpretation of the references to color in this figure legend, the reader is referred to the Web version of this article.)

numerical prediction of atmospheric processes and the inter-annual variability in meteorology when regional-scale air quality models are used.

Taking the baseline component of the ozone time series that is representative of the long-term variation dictated by emissions, policy changes, background, and trends, we apply the Baseline Projection Methodology in the context of attainment demonstration. The regression coefficients $a$ and $b$ of the BASE-GLO projection are estimated using a rank-ordered regression of the baseline between the BASE CMAQ simulation for 2010 as the base year and the GLO scenario simulation with 20% global reduction of anthropogenic emissions as the future year. Then, the same set of regression coefficients is employed to estimate the projected BL from observed BL in 2008, 2009 and 2010 (Step 1, Fig. 3; BL). Following Steps 2 and 3 in the methodology (see Fig. 3), we determine the distribution of the DV. The model simulations are used only to project the baseline making use of the linear relationship between the baseline in the base and the projected year anchored to the observed baseline. The observed DV in 2010 (Fig. 8a) shows widespread non-attainment of the 2015 ozone NAAQS of 70 ppb with some extreme high values at sites of southern California. The median DV for the BASE-GLO projection (Fig. 8c) shows a decrease of 3 ppb across all stations. This indicates the impact in the future DV across CONUS stemming from the 20% reduction in anthropogenic emissions. Whether this reduction is sufficient or not for attainment is determined from the probabilistic viewpoint of the 2015 NAAQS exceedances. With the median DV across all stations (71 ppb) above the

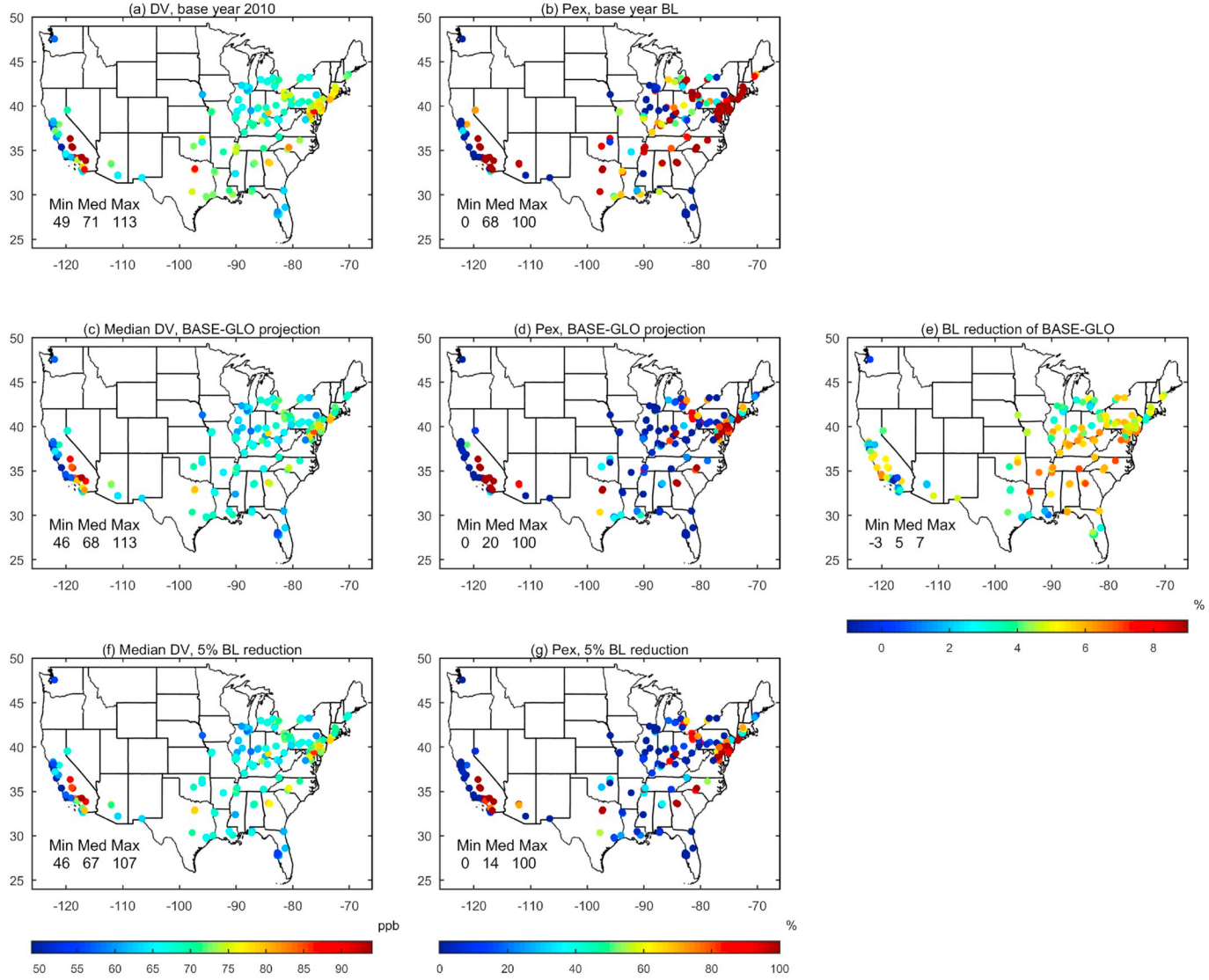


**Fig. 8.** Attainment demonstration with two emission control scenarios compared with base year conditions. Base case: (a) observed DV in base year 2010; (b) Pex (Probability of DV exceeding the 2015 ozone NAAQS of 70 ppb) with observed base year baselines. BASE-GLO emission control scenario: (c) median DV of the projected DV distribution; (d) Pex; (e) Percentage reduction of baseline mean from BASE to GLO. 5% BL reduction control scenario: (f) median DV of the projected DV distribution; (g) Pex.

2015 NAAQS in the base year 2010, the chance of the median DV exceeding 70 ppb is reduced from 68% to only 20% (Fig. 8b, d). It is apparent that this reduction is still not adequate for some areas, especially some California and Northeastern stations, to reach attainment (Fig. 8c and d). This BASE-GLO emission control scenario has a BL component reduction of around 5% nationwide with more prominent impacts in the Eastern US and central coastal area of California (Fig. 8e shows the reduction of the BL component from BASE to GLO).

When we apply a hypothetical 5% BL reduction scenario across the board (instead of using the model simulation reflecting the GLO scenario), the results are very similar to the BASE-GLO projection (Fig. 8f and g). This result indicates that a 5% BL reduction is approximately equivalent to a 20% anthropogenic emissions reduction GLO scenario. Given that the 5% BL reduction stemming from 20% emission reduction (i.e., GLO projection) is not adequate for attainment at many sites in California and NE US, we apply a hypothetical emission reduction scenario yielding in 15% baseline reduction in 2010 from some potential VOC and NOx emission control strategies. This reflects a stricter emission control scenario compared to the BASE-GLO case and the decrease in DV is more pronounced nationwide (Fig. 9). The probabilities of exceeding the NAAQS (Pex) are diminished for this stricter emission control scenario, except for some areas in California which still face non-attainment (see Fig. 9b).

Experimenting with various emission control scenarios that can be different for each region or state using regional air quality models by controlling sectors such as on-road NOx and industrial VOC or point source NOx or combinations of various emission sources provides a probabilistic assessment of non-attainment that is much more informative and robust than providing a simple “yes/no” answer on the efficacy of a control strategy to policy-makers. In other words, the proposed methodology enables the policy-makers to assess the probability of success in achieving the intended target with each envisioned emission control strategy. Ultimately, decisions pertaining to the selection of emission control strategies and the probability threshold for exceeding the ozone standard are the prerogatives of policy-makers.

## 5. Summary and conclusions

Prediction of the absolute pollutant concentration levels and changes in the peak ozone concentration values is challenging for

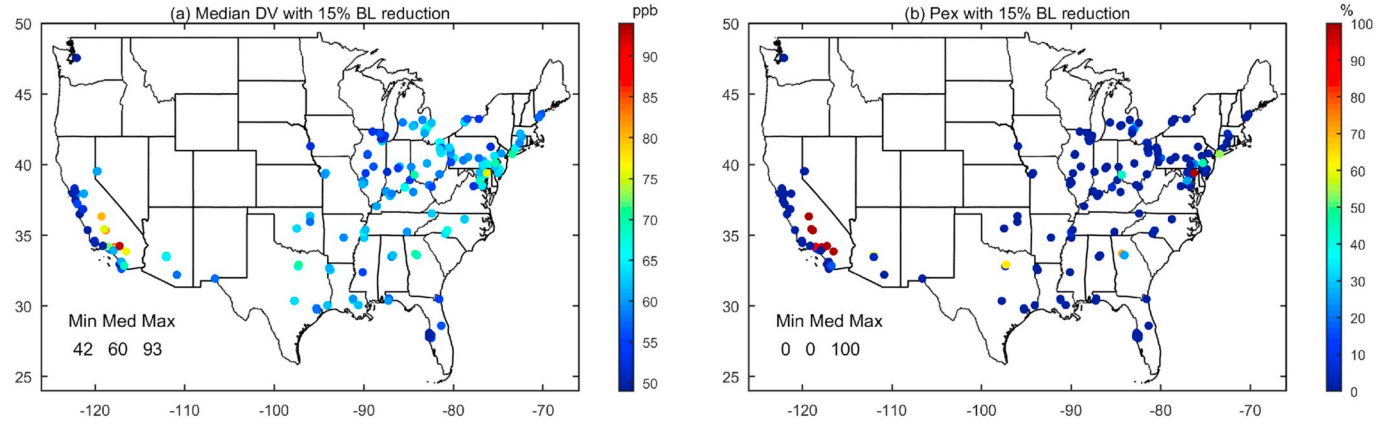


**Fig. 9.** Attainment demonstration with the 15% baseline reduction scenario: (a) median DV of the projected DV distribution and (b) Probability of DV exceeding the 2015 ozone NAAQS of 70 ppb.

regional air quality models because of uncertainties in input data as well as model physics and chemistry. Given the strong linkage between the magnitude of the baseline concentration level and peak ozone values, we developed a new method, namely the BL Projection, for estimating the associated 4th highest ozone, the design value and number of ozone exceedances and determine their confidence bounds by superimposing multi-decadal historical synoptic forcings acting on the prevailing BL concentration. This is demonstrated using 34-years of observations to establish the validity and robustness of the proposed methodology. As additional data become available in the future, the database for the synoptic forcings will expand beyond the 34 years used in this study, thereby facilitating more reliable and robust policy decisions on emissions management.

The use of the CMAQ model with the BL regression methodology is demonstrated using two simulations that share the same meteorological conditions (base case simulation for 2010 and 20% global anthropogenic emission reduction). Results indicate that the global 20% anthropogenic emission reduction yield a baseline change of only 5% across CONUS and is not adequate in some areas, especially stations in California and northeastern US. Thus, regulatory modeling assessments that focus on the impact of emission changes on the baseline ozone concentration level instead of on few high values of the ozone distribution would provide greater confidence in policy-making. Therefore, it is important that regional air quality models accurately simulate the baseline concentration and its changes stemming from emission reductions because it is the baseline component that strongly influences peak ozone levels or ozone exceedances. The BL Projection Method is easy to implement in the regulatory framework, thereby helping build confidence in the use of air quality models in the attainment demonstration process.

The key findings from the development and application of the probabilistic assessment of ozone exceedances are described below.

- Because all atmospheric models contain simplifications of the various physical and chemical processes occurring in the atmosphere and given the inherent parametric and structural uncertainties together with the stochastic nature of the atmosphere, we should not rely on modeled absolute pollutant concentration levels; it is often more useful to estimate the probability of the occurrence of an event rather than relying on a single best model result.
- The change in the long-term forcing from the base year stemming from a given emission reduction scenario when combined with the synoptic-scale weather fluctuations embedded in time series of historical ozone observations enables us to estimate the probability of exceeding the ozone standard associated with future emission reduction scenarios.
- Modeling results analyzed and presented in this probabilistic manner enable more explicit consideration of the ever-present uncertainty in projected changes in air quality needed to comply with the ozone standard.

## Acknowledgements

The views expressed in this paper are those of the authors and do not necessarily represent the view or policies of the U.S. Environmental Protection Agency. Two of the authors (MA and HL) gratefully acknowledge the support of this work by the Electric Power Research Institute (EPRI) Contract #00-10005071, 2015–2017.

## Appendix A. Supplementary data

Supplementary data to this article can be found online at https://doi.org/10.1016/j.atmosenv.2018.11.010.

## References

Astitha, M., Luo, H., Rao, S.T., Hogrefe, C., Mathur, R., Kumar, N., 2017. Dynamic evaluation of two decades of WRF-CMAQ ozone simulations over the contiguous United States. Atmos. Environ. 164, 102–116.
Chock, D.P., 1984. Statistics of extreme values of a first-order Markov normal process: an exact result. Atmos. Environ. 18, 2461–2470 1967.
David, H., 1981. Order Statistics. John Wiley, New York, pp. 8–22.
Emery, C., Liu, Z., Russell, A.G., Odman, M.T., Yarwood, G., Kumar, N., 2017. Recommendations on statistics and benchmarks to assess photochemical model performance. J. Air Waste Manag. Assoc. 67, 582–598.
Eskridge, R.E., Ku, J.Y., Rao, S.T., Porter, P.S., Zurbenko, I.G., 1997. Separating different scales of motion in time series of meteorological variables. Bull. Am. Meteorol. Soc. 78, 1473–1483.
Galmarini, S., Kioutsioukis, I., Solazzo, E., 2013. E pluribus unum*: ensemble air quality predictions. Atmos. Chem. Phys. 13, 7153–7182.
Galmarini, S., Koffi, B., Solazzo, E., Keating, T., Hogrefe, C., Schulz, M., Benedictow, A., Griesfeller, J.J., Janssens-Maenhout, G., Carmichael, G., Fu, J., Dentener, F., 2017. Technical note: Coordination and harmonization of the multi-scale, multi-model activities HTAP2, AQMEII3, and MICS-Asia3: simulations, emssion inventories, boundary conditions, and model output formats. Atmos. Chem. Phys. 17, 1543–1555. https://doi.org/10.5194/acp-17-1543-2017.
Gardner, M.W., Dorling, S.R., 2000. Meteorologically adjusted trends in UK daily maximum surface ozone concentrations. Atmos. Environ. 34, 171–176.
Gilliam, R.C., Hogrefe, C., Godowitch, J.M., Napelenok, S., Mathur, R., Rao, S.T., 2015. Impact of inherent meteorology uncertainty on air quality model predictions. J. Geophys. Res. Atmospheres 120 (12) 259–12,280.
Gumbel, E.J., 1958. Statistics of extremes. In: Statistics of Extremes. Columbia University, New York, pp. 75–155.
Guo, J.J., Fiore, A.M., Murray, L.T., Jaffe, D.A., Schnell, J.L., Moore, C.T., Milly, G.P., 2018. Average versus high surface ozone levels over the continental USA: model bias, background influences, and interannual variability. Atmos. Chem. Phys. 18 (16), 12123–12140.
Henneman, L.R.F., Liu, C., Hu, Y., Mulholland, J.A., Russell, A.G., 2017. Air quality modeling for accountability research: operational, dynamic, and diagnostic evaluation. Atmos. Environ. 166, 551–565.
Hogrefe, C., Liu, P., Pouliot, G., Mathur, R., Roselle, S., Flemming, J., Lin, M., Park, R.J., 2018. Impacts of different characterizations of large-scale background on simulated

regional-scale ozone over the continental United States. Atmos. Chem. Phys. 18, 3839–3864.
Hogrefe, C., Rao, S.T., 2001. Demonstrating attainment of the air quality standards: integration of observations and model predictions into the probabilistic framework. J. Air Waste Manag. Assoc. 51, 1060–1072.
Hogrefe, C., Rao, S.T., Kasibhatla, P., Hao, W., Sistla, G., Mathur, R., McHenry, J., 2001. Evaluating the performance of regional-scale photochemical modeling systems: Part II—ozone predictions. Atmos. Environ. 35 (24), 4175–4188.
Hogrefe, C., Rao, S.T., Zurbenko, I.G., Porter, P.S., 2000. Interpreting the information in ozone observations and model predictions relevant to regulatory policies in the eastern United States. Bull. Am. Meteorol. Soc. 81, 2083–2106.
Hogrefe, C., Roselle, S., Mathur, R., Rao, S.T., Galmarini, S., 2014. Space-time analysis of the air quality model evaluation international initiative (AQMEII) phase 1 air quality simulations. J. Air Waste Manag. Assoc. 64, 388–405.
Hogrefe, C., Vempaty, S., Rao, S.T., Porter, P.S., 2003. A comparison of four techniques for separating different time scales in atmospheric variables. Atmos. Environ. 37, 313–325.
Ibarra-Berastegi, G., Madariaga, I., Elías, A., Agirre, E., Uria, J., 2001. Long-term changes of ozone and traffic in Bilbao. Atmos. Environ. 35, 5581–5592.
Kang, D., Hogrefe, C., Foley, K.L., Napelenok, S.L., Mathur, R., Trivikrama Rao, S., 2013. Application of the Kolmogorov–Zurbenko filter and the decoupled direct 3D method for the dynamic evaluation of a regional air quality model. Atmos. Environ. 80, 58–69.
Maxwell-Meier, K.L., Chang, M.E., 2005. Comparison of ozone temporal scales for large urban, small urban, and rural areas in Georgia. J. Air Waste Manag. Assoc. 55, 1498–1507.
Milanchus, M.L., Rao, S.T., Zurbenko, I.G., 1998. Evaluating the effectiveness of ozone management efforts in the presence of meteorological variability. J. Air Waste Manag. Assoc. 48, 201–215.
Phalitnonkiat, P., Sun, W., Grigoriu, M.D., Hess, P., Samorodnitsky, G., 2016. Extreme ozone events: tail behavior of the surface ozone distribution over the U.S. Atmos. Environ. Times 128, 134–146.
Pinder, R.W., Gilliam, R.C., Appel, K.W., Napelenok, S.L., Foley, K.M., Gilliland, A.B., 2009. Efficient probabilistic estimates of surface ozone concentration using an ensemble of model configurations and direct sensitivity calculations. Environ. Sci. Technol. 43 (7), 2388–2393. https://doi.org/10.1021/es8025402. 2009.
Porter, P.S., Rao, S.T., Hogrefe, C., Gego, E., Mathur, R., 2015. Methods for reducing biases and errors in regional photochemical model outputs for use in emission reduction and exposure assessments. Atmos. Environ. 112, 178–188.
Porter, P.S., Rao, S.T., Hogrefe, C., Mathur, R., 2017. A reduced form model for ozone based on two decades of CMAQ simulations for the continental United States. Atmospheric Pollut. Res. 8, 275–284.
Rao, S.T., Porter, P.S., Mobley, J.D., Hurley, F., 2011. Understanding the spatio-temporal variability in air pollution concentrations. Environ. Manage. Nov 42–48.
Rao, S.T., Sistla, G., Pagnotti, V., Petersen, W.B., Irwin, J.S., Turner, D.B., 1985. Resampling and extreme value statistics in air quality model performance evaluation. Atmos. Environ. 19, 1503–1518 1967.
Rao, S.T., Zurbenko, I.G., 1994. Detecting and tracking changes in ozone air quality. Air Waste 44, 1089–1092.
Rao, S.T., Zurbenko, I.G., Neagu, R., Porter, P.S., Ku, J.Y., Henry, R.F., 1997. Space and time scales in ambient ozone data. Bull. Am. Meteorol. Soc. 78, 2153–2166.
Rao, S.T., Zurbenko, I.G., Porter, P.S., Ku, J.Y., Henry, R.F., 1996. Dealing with the ozone non-attainment problem in the Eastern United States. Environ. Manage. Jan 17–31.
Rao, S.T., Zalewsky, E., Zurbenko, I.G., 1995. Determining temporal and spatial variations in ozone air quality. J. Air Waste Manag. Assoc. 45, 57–61.
Roberts, E.M., 1979. Review of statistics of extreme values with applications to air quality data Part I. Review. J. Air Pollut. Contr. Assoc. 29, 632–637.
Sá, E., Tchepel, O., Carvalho, A., Borrego, C., 2015. Meteorological driven changes on air quality over Portugal: a KZ filter application. Atmospheric Pollut. Res. 6, 979–989.
Schere, K., Flemming, J., Vautard, R., Chemel, C., Colette, A., Hogrefe, C., Bessagnet, B., Meleux, F., Mathur, R., Roselle, S., Hu, R.-M., Sokhi, R.S., Rao, S.T., Galmarini, S., 2012. Trace gas/aerosol boundary concentrations and their impacts on continental-scale AQMEII modeling domains. Atmos. Environ., AQMEII: Int. Initiative Evaluation of Regional-Scale Air Quality Models - Phase 1 53, 38–50.
Solazzo, E., Bianconi, R., Hogrefe, C., Curci, G., Tuccella, P., Alyuz, U., Balzarini, A., Baró, R., Bellasio, R., Bieser, J., Brandt, J., Christensen, J.H., Colette, A., Francis, X., Fraser, A., Vivanco, M.G., Jiménez-Guerrero, P., Im, U., Manders, A., Nopmongcol, U., Kitwiroon, N., Pirovano, G., Pozzoli, L., Prank, M., Sokhi, R.S., Unal, A., Yarwood, G., Galmarini, S., 2017a. Evaluation and error apportionment of an ensemble of atmospheric chemistry transport modeling systems: multivariable temporal and spatial breakdown. Atmos. Chem. Phys. 17, 3001–3054.
Solazzo, E., Hogrefe, C., Colette, A., Garcia-Vivanco, M., Galmarini, S., 2017b. Advanced error diagnostics of the CMAQ and Chimere modelling systems within the AQMEII3 model evaluation framework. Atmos Chem Phys. Katlenburg-Lindau 17, 10435–10465.
U.S. EPA, 2014. Modeling Guidance for Demonstrating Attainment of Air Quality Goals for Ozone, PM2.5, and Regional Haze. December 2014 DRAFT available online at: https://www3.epa.gov/scram001/guidance/guide/Draft_O3-PM-RH_Modeling_Guidance-2014.pdf.
Vukovich, F.M., Sherwell, J., 2003. An examination of the relationship between certain meteorological parameters and surface ozone variations in the Baltimore–Washington corridor. Atmos. Environ. 37, 971–981.
Wise, E.K., Comrie, A.C., 2005a. Extending the Kolmogorov–Zurbenko filter: application to ozone, particulate matter, and meteorological trends. J. Air Waste Manag. Assoc. 55, 1208–1216.
Wise, E.K., Comrie, A.C., 2005b. Meteorologically adjusted urban air quality trends in the Southwestern United States. Atmos. Environ. 39, 2969–2980.
Yang, W., Zurbenko, I., 2010. Kolmogorov–Zurbenko filters. Wiley Interdiscip. Rev. Comput. Stat. 2, 340–351.
Zhang, Z., Ma, Z., Kim, S.-J., 2018. Significant decrease of PM2.5 in Beijing based on long-term 2 records and Kolmogorov–Zurbenko filter approach. Aerosol Air Qual. Res. 18, 711–718.
Zurbenko, I.G., Smith, D., 2018. Kolmogorov–Zurbenko filters in spatiotemporal analysis. Wiley Interdiscip. Rev. Comput. Stat. 10, e1419.